

Catalysts Used in Pollutant Ozonation

Subjects: Others

Contributor: Maria Victoria Ramon

The objective of this study was to summarize the results obtained in a wide research project carried out for more than 15 years on the catalytic activity of different catalysts (activated carbon, metal-carbon xerogels/aerogels, iron-doped silica xerogels, ruthenium metal complexes, reduced graphene oxide-metal oxide composites, and zeolites) in the photooxidation (by using UV or solar radiation) and ozonation of water pollutants, including herbicides, naphthalenesulfonic acids, sodium para-chlorobenzoate, nitroimidazoles, tetracyclines, parabens, sulfamethazine, sodium diatrizoate, cytarabine, and surfactants. All catalysts were synthesized and then texturally, chemically, and electronically characterized using numerous experimental techniques, including N₂ and CO₂ adsorption, mercury porosimetry, thermogravimetric analysis, X-ray diffraction, Fourier-transform infrared spectroscopy, Raman spectroscopy, X-ray photoelectron spectroscopy, diffuse reflectance UV-vis spectroscopy, photoluminescence analysis, and transmission electron microscopy. The behavior of these materials as photocatalysts and ozonation catalysts was related to their characteristics, and the catalytic mechanisms in these advanced oxidation processes were explored. Investigations were conducted into the effects on pollutant degradation, total organic carbon reduction, and water toxicity of operational variables and the presence of different chemical species in ultrapure, surface, ground, and wastewaters. Finally, a review is provided of the most recent and relevant published studies on photocatalysis and catalyzed ozonation in water treatments using similar catalysts to those examined in our project.

Keywords: Carbons ; catalysts ; photooxidation ; ozonation ; water pollutants ; UV radiation ; Solar radiation

1. Introduction

Advanced oxidation processes have been developed to increase the efficacy of ozone treatment based on the generation of HO[•] radicals^{[1][2]}. Solid catalysts have been proposed to increase the extent of ozonation^{[3][4]}. ACs, metal-doped carbon aerogels, and basic treated zeolites were studied.

2. Activated Carbons

AC is a promising ozonation catalyst because of its chemical and textural properties and low cost^{[5][6]}. The following groups of AC samples were studied for this purpose: (i) commercial ACs, (ii) ozonized ACs, (iii) nitrogen-enriched ACs, and (iv) ACs from petroleum coke.

The commercial ACs studied^[7] were Filtrasorb 400, Sorbo, Merck, Ceca GAC, Ceca AC40, Norit, and Witco, whose characteristics are reported in Table 1.

Table 1. Characterization of activated carbons (reproduced from^[7] with permission of Elsevier, 2002).

Activated Carbon	SN ₂ ^a	V ₂ ^b	V ₃ ^c	pH _{PZC}	Acid Groups ^d	Basic Groups ^e	Ash
	m ² /g	cm ³ /g	cm ³ /g		µeq/g	µeq/g	%
F400	1075	0.11	0.26	7.91	234	570	6.6
Sorbo	1295	0.06	0.37	9.42	88	1713	5.9
Merck	1301	0.09	0.26	7.89	114	582	5.2

Ceca GAC	966	0.13	0.16	6.83	323	99	12.0
Ceca AC40	1201	0.07	0.32	5.29	438	102	8.3
Norit	968	0.10	0.42	9.18	139	2050	4.8
Witco	808	0.04	0.05	6.85	183	253	0.3

^a Apparent surface area determined applying the BET equation to N₂ adsorption isotherm. ^b Volume of pores with a diameter of 50 to 6.6 nm. ^c Volume of pores with a diameter above 50 nm. ^d Determined by NaOH (0.1 N) neutralization. ^e Determined by HCl (0.02 N) neutralization.

The highest ash content (12%) was observed in Ceca GAC carbon and the lowest (0.3%) in Witco carbon (Table 1). High Fe (6.32%) and Al (8.41%) contents were found in Filtrasorb 400 ash, while Norit and Sorbo have low Fe and Al contents, but a substantive proportion of Mg and Ca (9–10% each). A high P content (4.11%) was observed in Ceca GAC alone. Ti was detected in Filtrasorb 400 and Merck ash samples at a concentration of @1% and Mn was found in Norit ashes at 0.25% and in Sorbo ashes at 0.13%. These metals often serve as catalysts in oxidation processes. Thus, Ti is favored as a catalyst in photocatalysis^[8], and low concentrations of MnO₂ were used by Ma and Graham^[9] to enhance chlorobenzene degradation by ozone.

Figure 1 shows the experimental results of NTS ozonation in the presence of the ACs, which all increase the ozonation rate. Sorbo, Norit, and Ceca GAC carbons produce a major increase in NTS degradation rate, whereas Witco AC has a lower effect. The higher NTS ozonation rate in the presence of these ACs may be attributable to an increased HO[•] concentration. The ozone-NTS direct reaction constant is 6.72 M⁻¹ s⁻¹, whereas the indirect reaction (free radical reaction) constant is 3.7 × 10⁹ M⁻¹ s⁻¹. Therefore, the radical reaction is more effective in oxidizing NTS. Similar results were obtained when these ACs were used in the ozonation of nitroimidazoles and surfactants^{[10][11][12]}.

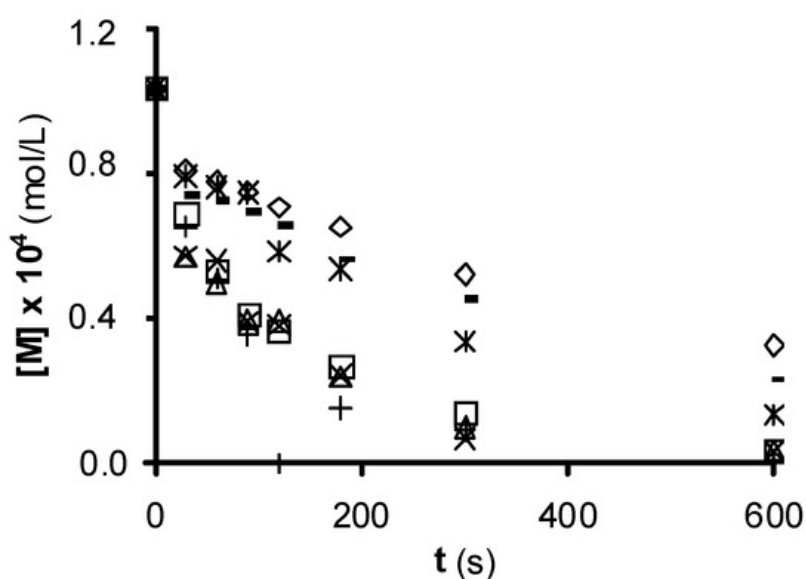
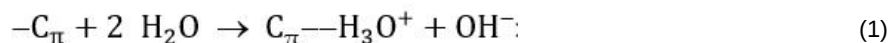


Figure 1. 1,3,6-naphthalentrisulfonic (NTS) ozonation in the presence of commercial activated carbon. (□), without carbon; (○), Filtrasorb 400; (△), Merck; (◇), Ceca GAC; (*), Ceca AC40; (◐), Norit; (+), Sorbo; (-) Witco (reproduced from^[13] with permission of John Wiley and Sons, 2003).

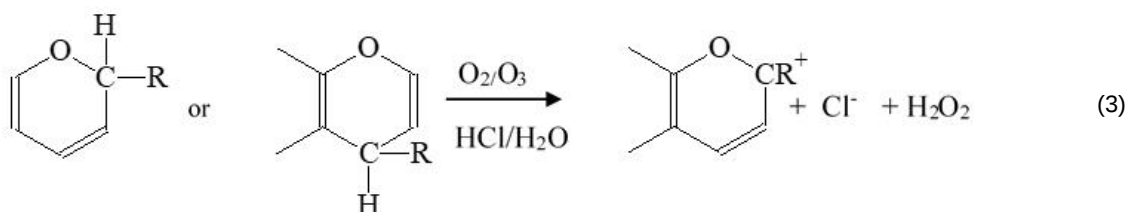
The ACs with the highest pH_{PZC} values and concentrations of basic surface groups produce the greatest increase in NTS ozonation rate (Table 1); however, this rate is not clearly related to the SN₂ of the AC. The most effective carbons to degrade NTS (Sorbo and Norit) have the largest volumes of macropores (Table 1), which behave as transport pores and favor the access of ozone to the carbon surface, reducing diffusion limitations. In this way, the low catalytic activity of Witco carbon may be in part attributable to their low V₂ and V₃ values.

ACs are heterogeneous materials with numerous surface groups and a variety of pore size distributions; however, the above findings indicate that their catalytic activity in NTS ozonation is largely a function of their basicity. Their basicity derives from the presence of basic oxygen-containing functional groups (e.g., pyrone or chromene) and/or graphene

layers acting as Lewis bases and forming electron donor–acceptor (EDA) complexes with H₂O molecules. The latter basic sites are localized at π electron-rich regions within the basal planes of carbon crystallites and away from their edges. This delocalized π electron system can act as a Lewis base in aqueous solution (reaction (1)):



Hence, the delocalized π electron system of basic carbons and oxygenated basic groups (chromene and pyrone) would behave as catalytic reaction centers and reduce ozone molecules to OH⁻ ion and hydrogen peroxide according to the following reactions:



Both OH⁻ and hydrogen peroxide act as initiators of ozone decomposition in aqueous phase^[14]. The presence of Sorbo (pH_{PZC} = 9.42) and Norit (pH_{PZC} = 9.18) produces higher NTS degradation rates because they have greater reducing properties, favoring reactions (2) and (3) and enhancing the decomposition of ozone into highly oxidative radicals.

The total NTS ozonation degradation rate in the presence of AC was considered as the sum of the homogeneous reaction rate in the absence of AC, $(-r_M)_{\text{homo}}$, and the heterogeneous reaction rate in the presence of AC, $(-r_M)_{\text{hetero}}$, mathematically expressed as:

$$(-r_{\text{total}}) = (-r_{\text{homo}}) + (-r_{\text{hetero}}) = \left(-\frac{dC_M}{dt}\right)_{\text{homo}} + \left(-\frac{dC_M}{dt}\right)_{\text{hetero}} \quad (4)$$

Heterogeneous reaction constants were determined as previously described^[15] (Table 2). Thus, k_{hetero} values can be considered as a measure of the catalytic activity of ACs in NTS ozonation.

Table 2. Heterogeneous reaction constants for original and demineralized ACs according to the proposed model (adapted from^[15] with permission of Elsevier, 2005).

Activated Carbon	k_{obs} s ⁻¹	k_{hetero} (mol/L) ⁻¹ s ⁻¹	$(k_{\text{hetero}})_{\text{demi}}$ (mol/L) ⁻¹ s ⁻¹
F400	0.0115	134.6	106.1
Sorbo	0.0152	189.4	142.3
Merck	0.1005	114.4	105.7
Ceca GAC	0.0155	195.2	90.4

Ceca AC40	0.0086	95.2	88.5
Norit	0.0653	210.5	190.4
Witco	0.0085	94.2	94.2

Study of the association between the k_{hetero} value (Table 2) and chemical characteristics (Table 1) of ACs revealed a greater increase in NTS degradation with ACs having a high ash content and elevated concentration of basic groups, which are both catalytic centers that can decompose the ozone into highly reactive species. The highest k_{hetero} values are observed in Norit, Sorbo, and Ceca GAC carbons.

Ozonation experiments were conducted in the presence of demineralized carbons to determine the contribution of the ash to the heterogeneous NTS ozonation rate. ACs were demineralized with HCl and HF, as previously described^[16]. As an example, results obtained for original and demineralized Ceca GAC samples are shown in Figure 2. The degradation rate is lower after demineralization in all ACs except for Witco because of its very low ash content (Table 1). These findings confirm the positive contribution of the mineral matter in ACs through their catalytic effect in NTS ozonation. All metals that have demonstrated catalytic activity in organic compound ozonation are found in the ACs under study, but the participation of each metal in the catalytic ozonation of NTS is difficult to evaluate.

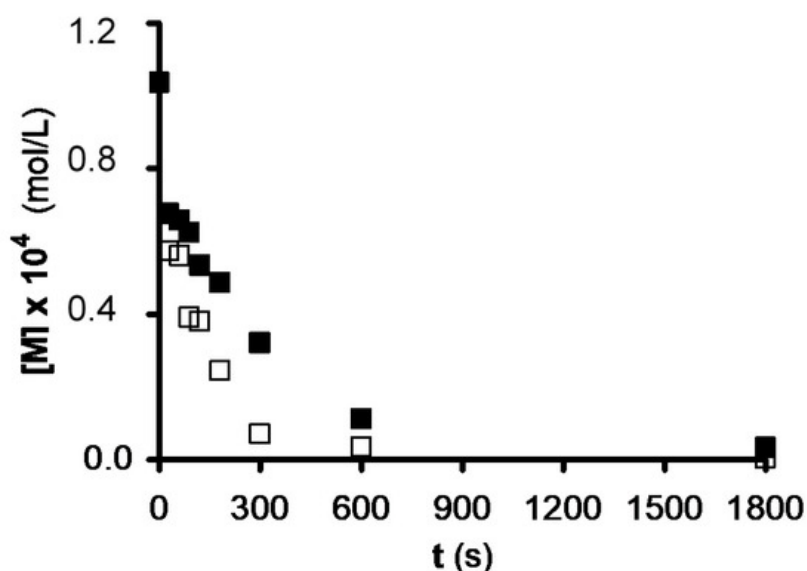


Figure 2. Effect of demineralization on the catalytic capacity of Ceca granulated activated carbon (GAC) carbon in NTS ozonation. pH = 2.3, T = 298 K. (■), untreated; (□), demineralized (reproduced from^[17] with permission of Elsevier, 2002).

It has been shown that the demineralization of carbons does not substantially affect their concentration of basic surface groups^[17], and the pH_{PZC} of the demineralized ACs is highly similar to that of the original ACs. Hence, a linear relationship was observed between their heterogeneous reaction constant and their surface concentration of basic groups (Figure 3). However, the ordinate in the origin is not zero, indicating that other features of the surface chemistry of ACs, in addition to the basic groups, contribute to their catalytic effect in NTS ozonation.

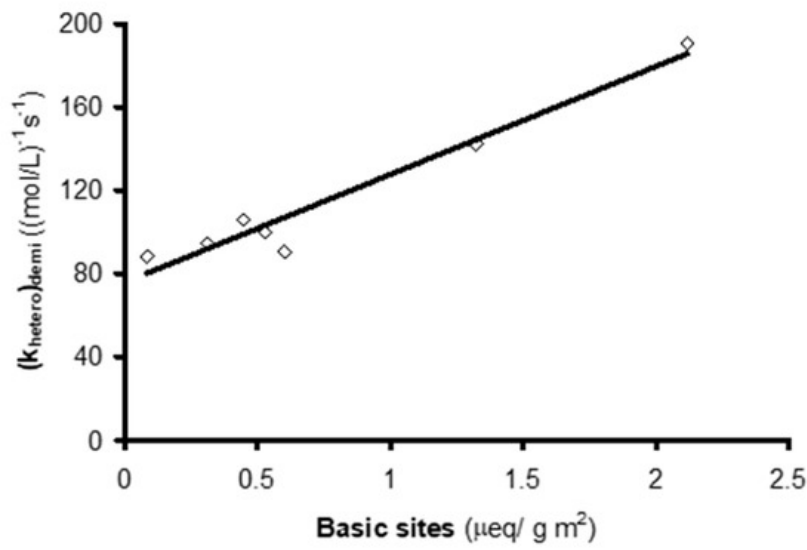


Figure 3. Relationship between $(k_{\text{hetero}})_{\text{demi}}$ value and concentration of basic groups on the activated carbons (reproduced from^[15] with permission of Elsevier, 2005).

In the presence of AC, ozonation can oxidize micropollutants by direct reaction with the ozone or by HO[•] radicals generated by the interaction of the ozone with the AC surface. The concentration of both oxidants must be known in order to calibrate this process with respect to its oxidation capacity. Previous studies have developed an experimental method for measuring concentrations of ozone and HO[•] radicals with conventional ozonation or with the AOP O₃/H₂O₂ ^[18]. The R_{ct} value is the ratio of HO[•] radical exposure to ozone exposure (Equation (5)).

$$R_{\text{ct}} = \frac{\int [\text{HO}^{\bullet}] dt}{\int [\text{O}_3] dt} \quad (5)$$

This ratio indicates the efficacy of ozone transformation into HO[•] radicals in a given system. The R_{ct} is calculated by measuring the reduction in a probe compound that reacts quickly with HO[•] but not ozone and by measuring the ozone concentration at the same time.

The influence of operational parameters was examined by conducting ozonation experiments in the presence of AC at ozone concentrations ranging between 2×10^{-5} and 6×10^{-5} M (1–3 mg/L) and AC doses ranging between 0.01 and 0.85 g/L^[19]. The efficacy of HO[•] radical formation was identified by adding sodium para-chlorobenzoate (pCBA) as HO[•] radical probe compound. pCBA has a low reactivity with ozone ($k_{\text{O}_3} = 0.15 \text{ M}^{-1} \text{ s}^{-1}$) and a high affinity for HO[•] radicals ($k_{\text{HO}^{\bullet}} = 5.2 \times 10^9 \text{ M}^{-1} \text{ s}^{-1}$).

The concentration of dissolved ozone in the system was evaluated because the potential to oxidize micropollutants is increased at high concentrations, which also augments the formation of oxidation byproducts, e.g., bromate^[20]. In addition, elevated O₃ exposure is required in disinfection systems, but not necessarily in systems designed to generate HO[•] radicals. Table 3 displays the R_{ct} values obtained in each experiment. It shows that this value is increased when AC F400 is present during pCBA ozonation, largely attributable to the increased rate constant for ozone decomposition (k_{D}), determined following a first-order kinetic model. Hence, the presence of AC promotes the transformation of ozone into HO[•] radicals, and a major increase in R_{ct} value is observed at higher concentrations of dissolved ozone in the O₃/AC system.

Table 3. R_{ct} values from experiments conducted at pH 7 in Milli-Q water ($[\text{NaH}_2\text{PO}_4] = 5 \times 10^{-3}$ M, $[\text{t-BuOH}] = 8 \times 10^{-5}$ M) (reproduced from^[19] with permission of Elsevier, 2005).

Experiment	Sample	Carbon Dose g/L	[O ₃] M	k _D s ⁻¹	R _{ct}
1	Without carbon	0.00	2×10^{-5}	6.0×10^{-4}	2.7×10^{-9}

2	F400	0.50	2×10^{-5}	3.2×10^{-3}	1.2×10^{-8}
3	F400	0.50	4×10^{-5}	3.6×10^{-3}	1.6×10^{-8}
4	F400	0.50	6×10^{-5}	4.0×10^{-3}	4.7×10^{-8}
5	F400	0.01	2×10^{-5}	6.1×10^{-4}	3.0×10^{-9}
6	F400	0.25	2×10^{-5}	9.0×10^{-4}	6.0×10^{-9}
7	F400	0.85	2×10^{-5}	8.0×10^{-3}	5.7×10^{-8}
10	F400-1	0.50	2×10^{-5}	2.9×10^{-3}	1.4×10^{-8}
11	F400-2	0.50	2×10^{-5}	2.6×10^{-3}	1.5×10^{-8}
12	F400-3	0.50	2×10^{-5}	2.4×10^{-3}	1.5×10^{-8}
13	F400-10	0.50	2×10^{-5}	1.0×10^{-3}	5.6×10^{-9}
14	F400-120	0.50	2×10^{-5}	4.0×10^{-4}	3.8×10^{-9}

It is important to determine the minimum AC dose needed to transform ozone into HO[•] radicals. A higher AC dose in the system also increases the pCBA oxidation rate, and a higher rate of ozone decomposition is observed when the AC dose is increased (Table 3, Experiments 2, 5–7). Plotting the k_D or R_{ct} values against the AC dose shows a large increase at higher doses. According to these findings, the dose of AC is a key factor in the transformation of ozone into HO[•] radicals.

Oxidation experiments were carried out with pre-ozonated ACs (F400-1, F400-2 and F400-3) to determine changes in AC activity during ozonation^[19]. It was observed that AC activity to transform ozone into HO[•] radicals is not affected by the ozone treatment applied, finding highly similar R_{ct} values for all three samples (Table 3, Experiments 2, 10–12). The behavior of the AC in prolonged ozone treatments was studied by subjecting AC samples to a much more drastic ozonation treatment (F400-10, F400-120). These ACs showed an important reduction in their activity to transform ozone into HO[•] radicals with a longer treatment time (Table 3, Experiments 2, 13, 14). The R_{ct} value is reduced from 1.2×10^{-8} (untreated) to 3.8×10^{-9} when the AC undergoes 120 min of gas-phase ozonation. According to these findings, ozone oxidation decreases the AC's catalytic properties by increasing the number of acidic oxygenated surface functional groups^[19]. The electronic density of the graphene layers is diminished by these (electron-withdrawing) groups, decreasing its reductive properties and reactivity with ozone. Hence, it appears that the AC is not a true catalyst for ozone transformation but behaves as a conventional initiator or promoter in the transformation of ozone into HO[•] radicals.

As already noted, the combination of ozone and AC is an appealing technique for removing toxic organic compounds from waters through the AC's capacity to transform ozone into HO[•] radicals with higher oxidant power. This capacity is related to the AC's porous texture, surface chemistry (basic groups), and mineral matter. Accordingly, AC from petroleum coke and nitrogen-enriched ACs were prepared in our laboratory to enhance ozone transformation into HO[•] radicals^{[21][22]}.

Petroleum coke is a residue of the petrochemical industry, with around 4 tons being produced in the refining of 100 tons of crude oil. It cannot be used in production processes due to its elevated concentration of heavy metals (Ni, V, Fe), but this feature means that petroleum coke is an attractive material for utilization in the ozonation of aromatic pollutants. Table 4 shows the results of the textural characterization of the ACs prepared with different KOH/coke mass ratios, showing that the porosity of all samples is markedly developed by their activation, augmenting the volume of micro- (V_{mic}), meso- (V_2), and macropores (V_3). Activation of the coke also modifies its chemical nature (Table 4). Thus, the original material is mildly acid ($pH_{pZC} = 6.5$), whereas the pH_{pZC} of KOH-activated coke ranges from 8.4 for sample C-1 to 9.7 for sample C-4. This is largely due to the generation of basic surface groups during the activation process, which increases with a higher KOH/coke ratio.

Table 4. Textural characterization of original and activated cokes (adapted from^[22] with permission of Elsevier, 2006).

Sample	KOH/Coke	SN ₂	V _{mic}	V ₂ ^a	V ₃ ^b	pH _{PZC}
		m ² /g	cm ³ /g	cm ³ /g	cm ³ /g	
C	0	<30	0.02	Nil	0.011	6.5
C-1	1	1619	0.55	0.063	0.132	8.4
C-2	2	1261	0.41	0.061	0.154	8.8
C-3	3	1021	0.25	0.058	0.176	9.3
C-4	4	970	0.20	0.051	0.263	9.7

V_{mic} = micropore volume determined applying Dubinin–Radushkevich equation to CO₂ adsorption isotherm. ^a Volume of pores with a diameter of 50 to 6.6 nm. ^b Volume of pores with a diameter above 50 nm.

The k_{hetero} value of each carbon sample was calculated to determine the increase in NTS ozonation produced by its presence (Table 5), showing that the chemical activation process increases the activity of petroleum coke in NTS ozonation. Thus, the increase in k_{hetero} values with respect to that of the original coke ranges from 83% for sample C-1 to 16% for sample C-4, mainly by developing the porosity of the coke, which increases access of the ozone to its active surface sites and mineral matter, and by increasing the surface basicity of the original coke, which favors ozone reduction on its surface and thereby enhances its transformation into highly oxidant species.

Table 5. Heterogeneous reaction rate constants of activated coke samples in NTS ozonation (adapted from^[22] with permission of Elsevier, 2006).

Sample	C	C-1	C-2	C-3	C-4
k _{hetero} (mol/L) ⁻¹ s ⁻¹	57.7	105.8	86.5	76.9	67.3

Ozonation modifies the oxygenated surface groups and metal sites of these ACs and can change their oxidation state. The Fe 2p_{3/2} spectrum for samples C-1 and C-1-ozonated shows a 14% increase in the surface concentration of Fe₂O₃ on C-1-ozonated. According to these findings, the ozone can attack Fe(II) metal sites on the carbon surface during NTA ozonation, generating Fe(III) by Equations (6) and (7). These reactions can also enhance ozone transformation rate into HO[•] radicals, contributing to the ozonation of NTS. The main mineral components are Ni and V, and the Ni 2p_{3/2} and V 2p_{3/2} spectra show no modification in their initial oxidation state (Ni in oxidation state +2 and V in oxidation state +5).



ACs enriched in basic surface groups were prepared to examine their efficacy for NTS removal^[21]. The basic surface groups were generated by treating Witco AC with nitrogenating agents (urea, ammonia, or ammonium carbonate); the textural characteristics of the samples obtained are displayed in Table 6. The treatments augment the surface area of carbon W (SN₂), especially the urea treatment (W-U). W-U has increased microporosity due to its gasification by the urea. Table 6 also reports the pore volume values determined by mercury porosimetry (V₂ and V₃), showing that treatment with ammonia (W-A) or ammonium carbonate (W-C) produces a low development of the meso- and macroporosity, whereas treatment with urea produces a high development of the micro-, meso-, and macroporosity.

Table 6. Textural characterization of basic activated carbon samples (adapted from^[21] with permission of American Chemical Society, 2004).

Sample	SN ₂ m ² /g	V _{micro} cm ³ /g	V ₂ cm ³ /g	V ₃ cm ³ /g
W	812	0.238	0.040	0.050
W-A	904	0.206	0.047	0.091
W-C	825	0.222	0.042	0.102
W-U	1057	0.289	0.064	0.122

Study of the catalytic activity of the AC samples in NTS ozonation revealed increased activity in the basic samples. In the sample with the highest catalytic activity (W-U), a large proportion of surface nitrogenated groups are pyrrole groups, and a small proportion is pyridine groups, indicating that AC catalytic activity is enhanced by pyrrole-type groups. This may have the following explanation: the pair of nitrogen electrons in the pyrrole group form part of the ring electronic cloud and are therefore delocalized among the five atoms of the molecule. Consequently, pyrrole has 6 π electrons on 5 centers, making them π -excessive aromatic rings. Hence, the presence on the AC surface of pyrrole groups increases the electronic density of its basal plane, increasing its capacity to reduce the ozone dissolved on its surface (reaction (2)).

In addition, the increase in the π electron system of the AC produced by the pyrrole groups enhances the interaction with the water molecules (reaction (1)). Both processes generate OH⁻ ions in the solution, and these behave as initiators of the ozone decomposition into HO[•] radicals, highly reactive against NTS, which increases the degradation rate (reactions (8)–(10)).

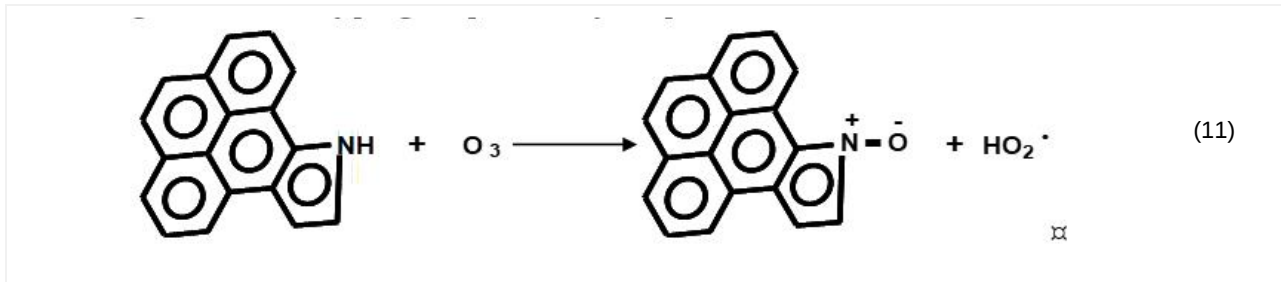


A study was conducted on the transformation of nitrogen functional groups from an interaction between ozone and AC surface during NTS ozonation in order to determine their involvement in the catalytic activity. As an example, Table 7 exhibits the changes observed in sample W-U, showing that pyridone groups are not affected by ozonation, but a large number of pyrrole-type groups are oxidized and transformed into N-oxide-type groups.

Table 7. Effect of ozonation on the concentration (%) of nitrogen surface groups on the urea treatment sample (W-U) (reproduced from^[21] with permission of American Chemical Society, 2004).

Sample	Pyridine (398.5 ± 0.2 eV)	Pyridone (399.5 ± 0.2 eV)	Pyrrole (400.5 ± 0.2 eV)	N-oxide (402.5 ± 0.2 eV)
W-U	8	42	50	-

According to these findings, ozone can attack the pyrrolic groups of AC graphene planes during ozonation, resulting in N-oxide type groups and hydroperoxide radicals (reaction (11)).



This reaction accounts for the changes in the pyrrole group during ozonation, which would contribute to NTS ozonation because the hydroperoxide radical increases the decomposition of ozone into radicals that can effectively degrade NTS. This may contribute to the higher catalytic activity of pyrrole groups on the AC surface.

3. Metal-Doped Carbon Aerogels

As mentioned above, the chemical and textural characteristics of carbon aerogels and their ready preparation have led to their utilization in numerous industrial applications^{[23][24][25]}. Thus, carbon aerogels show high promise for boosting ozone transformation into HO[•] radicals by taking advantage of the properties of transition metals, which have contrasting catalytic activities during ozonation, preventing their dissolution in the medium and separation from the system.

Table 8 exhibits the textural characteristics of the original aerogels (A, A-Co(II)-15, A-Mn(II)-15, and A-Ti(IV)-15) prepared for utilization as ozonation catalysts^{[26][27]}. They all have a much larger volume of mesopores (diameter 6.6–50 nm) (V_2) and macropores (V_3) than of micropores (V_{mic}).

Table 8. Textural characterization of basic activated carbon samples (adapted from^[26] with permission of Elsevier, 2006).

Sample	SN ₂ m ² /g	SCO ₂ m ² /g	V _{micro} cm ³ /g	V ₂ cm ³ /g	V ₃ cm ³ /g
A	500	200	0.07	0.36	0.68
A-Co(II)-15	562	206	0.07	0.43	0.97
A-Ti(IV)-15	550	203	0.07	0.40	0.92
A-Mn(II)-15	554	210	0.07	0.41	0.95
A-Mn(II)-15-1	540	200	0.07	0.41	0.94
A-Mn(II)-15-2	534	204	0.07	0.40	0.93
A-Mn(II)-15-3	546	206	0.07	0.41	0.95
A-Co(II)-15-1	560	210	0.07	0.41	0.92
A-Ti(IV)-15-1	538	200	0.07	0.38	0.90

Some chemical characteristics of carbon aerogels are shown in Table 9. Textural analysis of aerogel samples treated with ozone (A-Mn(II)-15-1, A-Mn(II)-15-2, A-Mn(II)-15-3, A-Co(II)-15-1 and A-Ti(IV)-15-1) showed similar SN_2 , SCO_2 , V_2 , and V_3 values to those in the non-pretreated samples (Table 8). According to XPS analysis, all samples show an increased percentage of surface oxygen with a higher number of ozonation cycles, whereas their pH_{PZC} values remain similar to initial values ($pH_{PZC} = 3-4$). The surface oxygen groups produced during ozonation is largely in the form of $-C=O$ in all aerogel samples. Interestingly, Mn(III) and Mn(IV) are formed in the O_3 -pretreated Mn-doped aerogel sample, and the percentage of Mn in oxidation state +4 increases with more pretreatment ozonation cycles. In samples A-Co(II)-15-1 and A-Ti(IV)-15-1, however, the oxidation state of Co and Ti stays at +2 and +4, respectively, after ozonation (Table 9).

Table 9. Chemical characterization of the aerogel samples (adapted from^[26] with permission of Elsevier, 2006).

Sample	pH_{PZC}	C	O	Co(II)	Mn(II)	Mn(III)	Mn(IV)	Ti(IV)
		%	%	%	%	%	%	%
A	3.5	68	32	-	-	-	-	-
A-Co(II)-15	3.8	64	22	14	-	-	-	-
A-Ti(IV)-15	4.3	64	21	-	-	-	-	15
A-Mn(II)-15	4.2	62	22	-	16	-	-	-
A-Mn(II)-15-1	4.0	54	30	-	10	4	2	-
A-Mn(II)-15-2	4.1	49	35	-	8	4	4	-
A-Mn(II)-15-3	3.9	42	42	-	6	4	6	-
A-Co(II)-15-1	3.9	55	31	14	-	-	-	-
A-Ti(IV)-15-1	4.2	53	32	-	-	-	-	15

Table 10 displays the R_{ct} values for pCBA ozonation in the presence of carbon aerogels and the corresponding ozone decomposition constants (k_D) determined by a first-order kinetic model.

Table 10. Determination of R_{ct} value in the different ozonation experiments: pH 7, T 25 °C, $[O_3] = 2 \cdot 10^{-5}$ M, $[pCBA] = 8 \cdot 10^{-5}$ M) (adapted from^[26] with permission of Elsevier, 2006).

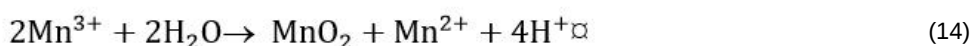
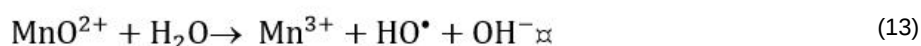
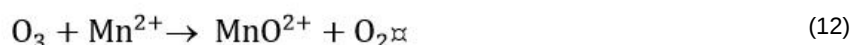
Experiment	Sample	Carbon Dose	k_D	R_{ct}
		mg	s^{-1}	
1	Without aerogel	0	$6.0 \cdot 10^{-4}$	$2.68 \cdot 10^{-9}$
2	A	2.5	$6.2 \cdot 10^{-4}$	$2.74 \cdot 10^{-9}$
3	A-Co(II)-15	2.5	$5.8 \cdot 10^{-4}$	$2.56 \cdot 10^{-9}$

4	A-Ti(IV)-15	2.5	6.1×10^{-4}	2.73×10^{-9}
5	A-Mn(II)-15	2.5	4.2×10^{-3}	5.36×10^{-8}
10	A-Mn(II)-15-1	2.5	2.6×10^{-3}	3.35×10^{-8}
11	A-Mn(II)-15-2	2.5	2.1×10^{-3}	2.68×10^{-8}
12	A-Mn(II)-15-3	2.5	1.4×10^{-3}	1.78×10^{-8}

pCBA removal is not enhanced by the presence of the blank aerogel (sample A), and R_{ct} and k_D values are similar to those obtained with no aerogel (Table 10). Hence, the organic matrix of the aerogel does not contribute to the ozone transformation into HO^\bullet radicals. The presence of Mn aerogel increases the pCBA removal rate, whereas that of Co- or Ti-doped carbon aerogels has practically no impact. Given the slow reactivity of pCBA against ozone^[28] and the slow adsorption kinetics of pCBA on the aerogel samples^[26], the generation of HO^\bullet radicals in the system would be largely responsible for the increased oxidation rate in the presence of Mn aerogel. Furthermore, the lack of an increase in pCBA removal when the blank (aerogel A) is present corroborates a direct relationship between the activity of the aerogels to transform ozone into HO^\bullet radicals and the presence of the metal on their surfaces.

R_{ct} values are 20-fold higher when the Mn aerogel is present during pCBA ozonation, but those obtained when Co(II) or Ti(IV) are present are similar to the R_{ct} values observed when they are not. The presence of Mn(II) aerogel during pCBA ozonation also increases the k_D value, but the presence of Co(II) or Ti(IV) aerogels has practically no effect (Table 10, Experiments 2–5). These results confirm that ozone transformation into HO^\bullet radicals is enhanced by the presence of Mn-doped carbon aerogel during the ozonation.

The mechanism by which the Mn(II) aerogel accelerates the pCBA removal rate was examined by XPS analysis of samples A-Co(II)-15, A-Mn(II)-15, and A-Ti(IV)-15 after their ozonation (samples A-Co(II)-15-1, A-Mn(II)-15-1, and A-Ti(IV)-15-1). Tables 8 and 9 exhibit their textural and chemical characteristics. Notably, the sample that enhances ozone transformation into HO^\bullet radicals (A-Mn(II)-15) is the one showing a post-ozonation increase in oxidation state (Table 9). On this sample, 10% of the surface Mn is in Mn(II), 4% in Mn(III), and 2% in Mn(IV) forms. However, the oxidation states of Co and Ti (samples A-Co(II)-15 and A-Ti(IV)-15) are not changed by ozonation (+2 and +4, respectively). According to these findings, the mechanism underlying the effect of the A-Mn(II)-15 aerogel on ozone transformation into HO^\bullet radicals is based on oxidation–reduction reactions. Hence, in agreement with results in Tables 9 and 10, the following reactions may be responsible for accelerating this transformation in the presence of A-Mn(II)-15 aerogel during pCBA:



Therefore, ozone transformation into HO^\bullet radicals through the oxidation of surface Mn(II) to Mn(III) and Mn(IV) during the oxidation process accounts for the increased pCBA removal rate. This agrees with the mechanism proposed by other authors^{[29][30]} for atrazine and oxalic acid ozonation in the presence of dissolved Mn(II) and MnO_2 .

4. Basic Treated Zeolites

The crystalline network of zeolites, which are aluminosilicates, has cavities containing large ions and water molecules. Their widely varied chemical and structural composition and regular porosity make them ideal adsorbents and/or catalysts^[31]. Zeolites have been proposed as catalysts of ozone decomposition in water and have been found to increase the production of free radicals during ozonation, which may be responsible for the removal of micropollutants from water^{[32][33][34]}. There is currently no consensus on the factors that influence these processes, including the catalytic activity of the metals in zeolites or the ozone concentration of the catalyst. Therefore, we studied ozonation of the anionic surfactant sodium dodecylbenzene sulfonate (SDBS) as a model pollutant^[35], determining the consumption of ozone and degradation of SDBS with the corresponding rate constants. Based on these findings, we proposed a reaction mechanism to modify these materials for treatment optimization.

Three types of zeolites were studied, one prepared in our lab and two commercial zeolites: high-silica zeolite ZSM-5 ($\text{SiO}_2/\text{Al}_2\text{O}_3$ ratio of 1000, CAS 308081-08-5), supplied by Acros Organics, and zeolite Z-13X ($\text{Na}_{86}[\text{AlO}_2]_{86}(\text{SiO}_2)_{106} \cdot x\text{H}_2\text{O}$, CAS 63231-69-6), supplied by Sigma-Aldrich. Zeolite Z-2 was obtained by mixing a molar ratio of 1.51 Na_2O , 1.13 Al_2O_3 , 0.26 SiO_2 , and 17 H_2O (Si/Al theoretical ratio = 0.24) and heating for 2 h at 373 K. Tables 11 and 12 summarize the crystallographic, elemental, and textural characteristics of all samples.

Table 11. Textural characteristics of zeolites (reproduced from^[35] with permission of Elsevier, 2012).

Sample	SN_2	$W_0(\text{N}_2)^a$	$W_0(\text{CO}_2)^b$	$L_0(\text{N}_2)^c$	$L_0(\text{CO}_2)^d$
	m^2/g	cm^3/g	cm^3/g	nm	nm
Z-2	7.1	0.037	0.144	2.02	1.00
Z-13X	341.3	0.166	0.184	0.48	0.30
ZSM-5	314.4	0.161	0.245	0.41	0.74
ZSM-5-NaOH	326.4	0.162	0.320	0.70	1.14

^a Volume of micropores obtained from the Dubinin–Radushkevich equation applied to N_2 adsorption data. ^b Volume of micropores obtained from the Dubinin–Radushkevich equation applied to CO_2 adsorption data. ^c Average micropore width obtained from N_2 adsorption isotherms. ^d Average micropore width obtained from CO_2 adsorption isotherms.

Table 12. Chemical characteristics of zeolites (reproduced from^[35] with permission of Elsevier, 2012).

Sample	Composition (%)				pH_{PzC}	Si/Al
	Zeolite-A	Sodalite	ZSM-5	Faujasite		
Z-2	97.3	2.7	0	0	11.4	0.89
Z-13X	0	0	0	100	11.1	1.73
ZSM-5	0	0	100	0	2.8	598.50
ZSM-5-NaOH	0	0	100	0	7.3	394.44

SDBS removal during ozonation in the presence and absence of the original zeolites is depicted in Figure 4, and the time course of ozone consumption in Figure 5. SDBS removal and ozone consumption rate constants are displayed in Table 13. According to these findings, Z-13X and Z-2 produced a small increase and ZSM-5 a small reduction in the SDBS removal rate. The increased SDBS removal in the presence of zeolites is related to the higher ozone consumption

observed during O₃/Zeolite treatment. Ozone has low reactivity with SDBS by direct reaction ($k_{O_3} = 3.67 \text{ M}^{-1} \text{ s}^{-1}$ [36]); therefore, SDBS degradation is largely due to the generation of HO[•] radicals during ozone decomposition [148]. The reaction constant of HO[•] radicals with SDBS is elevated ($k_{HO^{\bullet}} = 1.16 \cdot 10^{10} \text{ M}^{-1} \text{ s}^{-1}$ [36]), explaining the quick and effective degradation of the surfactant.

Figure 4 shows that SDBS removal in these systems diminishes in the order: O₃/Z-13X > O₃/Z-2 > O₃ > O₃/ZSM-5. Therefore, the highest removal rate is obtained by the most basic zeolite with the largest surface area, Z-13X, underscoring the important role of these parameters in the efficacy of a zeolite as an ozone decomposition catalyst for the generation of HO[•] radicals. ZSM-5 obtained the lowest rate, attributable to its acid character and greater capacity to stabilize dissolved ozone molecules. However, the consumption of ozone in the presence of SDBS (Figure 5) is more rapid with the O₃/ZSM-5 than with the O₃/Z-2 system. This behavior can be attributed to the two possible contributions of zeolite to ozone consumption: (i) adsorptive contribution (reaction (15)), mainly influenced by its hydrophobicity and the type and development of its porous texture; and (ii) catalytic contribution (reaction (16)), which depends on its basicity.

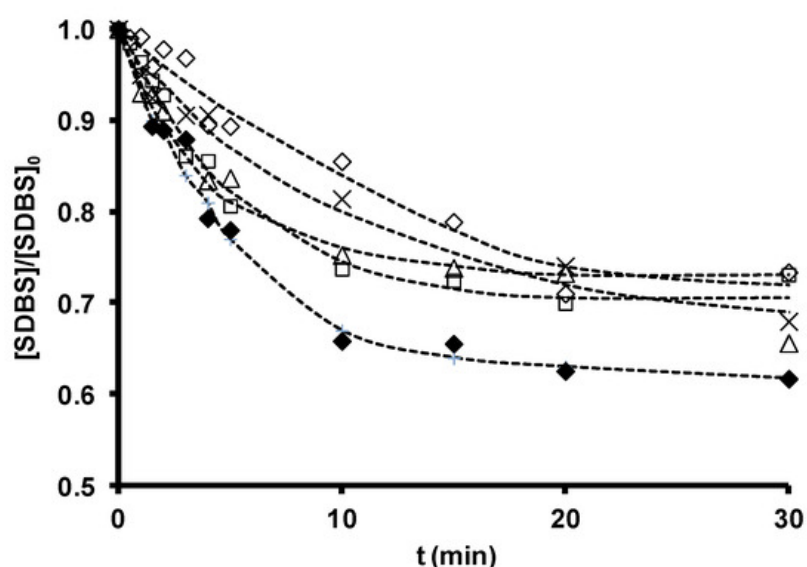
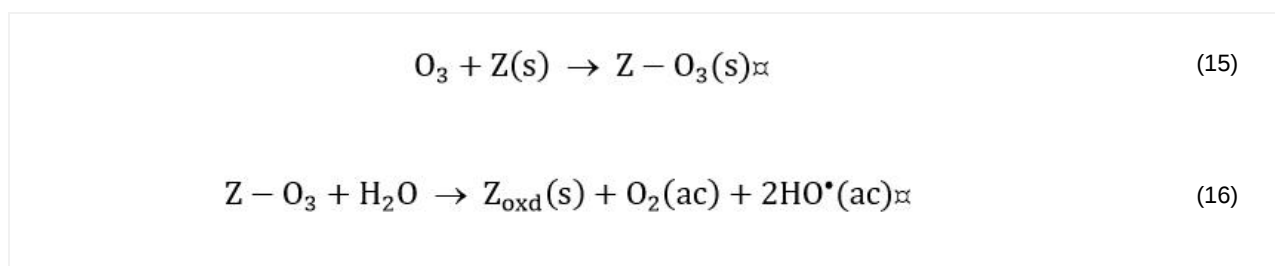


Figure 4. Sodium dodecylbenzene sulfonate (SDBS) removal as a function of ozonation time in the presence of zeolites. $[SDBS]_0 = 2.8 \cdot 10^{-5} \text{ M}$, $T = 298 \text{ K}$, $[O_3] = 2 \cdot 10^{-5} \text{ M}$, $[zeolite] = 100 \text{ mg/L}$. (x), O₃; (Δ), O₃/Z-2; (□), O₃/ZSM-5; (E), O₃/Z-13X; (◆), O₃/ZSM-5-NaOH. (- -) Fitted trend (reproduced from [35] with permission of Elsevier, 2012).

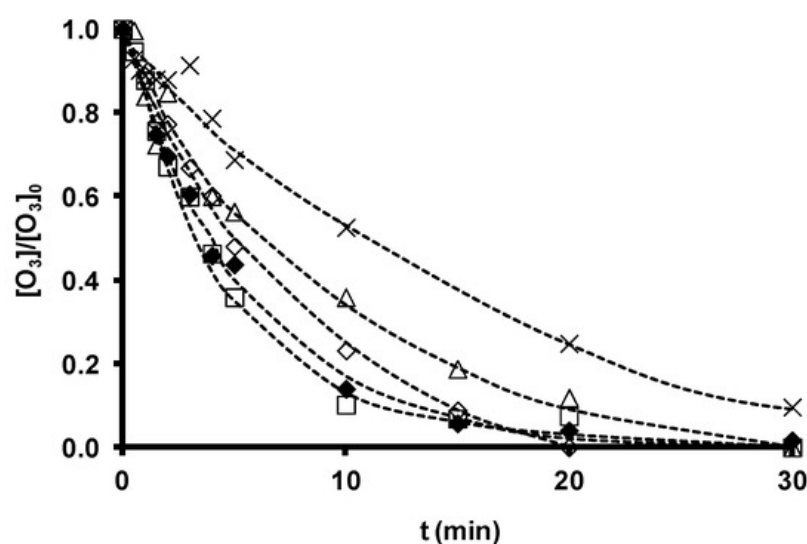


Figure 5. Time course of ozone concentration as a function of ozonation time in the presence of zeolites with different chemical characteristics. $[SDBS]_0 = 2.8 \times 10^{-5}$ M, T 298 K, $[O_3] = 2 \times 10^{-5}$ M, [zeolite] = 100 mg/L. (×), O_3 ; (Δ), $O_3/Z-2$; (□), $O_3/ZSM-5$; (£), $O_3/Z-13X$; (◆), $O_3/ZSM-5-NaOH$. (—) Fitted trend (reproduced from^[35] with permission of Elsevier, 2012).

Table 13. Ozone consumption and SDBS removal rate constants (reproduced from^[35] with permission of Elsevier, 2012).

Zeolite	Dose	$K_{obs}(O_3)$	R^2	$K_{obs}(SDBS)$	R^2	$(CHO^*)_{het}$
	mg/L	$s^{-1} \times 10^3$		$s^{-1} \times 10^4$		mol/L $\times 10^{15}$
Without zeolite	0	1.27 ± 0.04	0.997	2.75 ± 0.66	0.971	
Z-2	100	1.73 ± 0.17	0.984	4.05 ± 1.16	0.959	1.36
Z-13X	100	3.83 ± 0.28	0.993	7.36 ± 1.16	0.975	4.61
ZSM-5	100	2.50 ± 0.21	0.993	2.69 ± 0.37	0.983	0
ZSM-5-NaOH	100	3.24 ± 0.22	0.981	6.25 ± 1.66	0.965	3.55

The hydrophobicity of the zeolite in the $O_3/ZSM-5$ system is high and the basicity low, accelerating the consumption of ozone by adsorption. The stabilization of ozone on the adsorbent surface hampers the formation of HO^* radicals and, therefore, the degradation of SDBS. In contrast, the adsorbent hydrophobicity of the zeolite is low in the $O_3/Z-13X$ and $O_3/Z-2$ systems, and its basicity is high, increasing the decomposition of ozone and generation of radicals. These HO^* radicals participate in ozone decomposition in the presence of SDBS ($k_{O_3} = 1 \times 10^8 - 2 \times 10^9$ M⁻¹ s⁻¹ ^[37]) (reaction (17)) and react with and degrade SDBS (reaction (18)). Consequently, ozone consumption is reduced in these systems in the presence of SDBS. This increases the efficacy of the system because fewer of the generated radicals are involved in the chain mechanism of ozone decomposition (reaction (17)).



In order to increase the catalytic potential of acid zeolite ZSM-5 in SDBS degradation, SDBS ozonation experiments were conducted in the presence of NaOH-activated ZSM-5 (sample ZSM-5-NaOH); Figures 4 and 5, and Table 13 exhibit the results.

Figure 4 shows a major increase in SDBS degradation rate (125% increase in k_{SDBS}) with the NaOH-modified zeolite ZSM-5-NaOH versus the untreated zeolite, but an increase of only 29.6% in ozone consumption (Table 13). According to findings on the chemical and textural characteristics of the samples (Tables 11 and 12), treatment of ZSM-5 with NaOH produces: (i) increased basicity (increased pH_{pzc}), (ii) widened microporosity, and (iii) reduced hydrophobicity. These changes favor ozone decomposition into HO^* radicals and, therefore, SDBS degradation. As shown in Table 13, an increased concentration of HO^* radicals $(CHO^*)_{het}$ available for micropollutant oxidation is produced when Z13-X and ZSM5-NaOH are present during SDBS ozonation.

References

1. Bruny, R.; Bourbigot, M.M.; Doré, M. Oxidation of organic compounds through the combination ozone-hydrogen peroxide. *Ozone Sci. Eng.* 1985, 7, 241–257.
2. Beltrán, F.J.; García Araya, J.F.; Acedo, B. Advanced oxidation of atrazine in water. II Ozonation combined with ultraviolet radiation. *Water Res.* 1994, 28, 2165–2174.

3. Logemann, F.P.; Anne, J.H.J. Water treatment with a fixed bed catalytic ozonation process. *Water Sci. Technol.* 1997, 35, 353–360.
4. Jans, U.; Hoigné, J. Activated carbon and carbon black catalyzed transformation of aqueous ozone into oh-radicals. *Ozone Sci. Eng.* 1998, 20, 67–90.
5. Sheng H Lin; Cheng L Lai; Kinetic characteristics of textile wastewater ozonation in fluidized and fixed activated carbon beds. *Water Research* 2000, 34, 763-772, [10.1016/S0043-1354\(99\)00214-6](https://doi.org/10.1016/S0043-1354(99)00214-6).
6. Pedro M. Álvarez; J.F. García-Araya; F.J. Beltrán; I. Giráldez; J. Jaramillo; V. Gómez-Serrano; The influence of various factors on aqueous ozone decomposition by granular activated carbons and the development of a mechanistic approach. *Carbon* 2006, 44, 3102-3112, [10.1016/j.carbon.2006.03.016](https://doi.org/10.1016/j.carbon.2006.03.016).
7. J. Rivera-Utrilla; Manuel Sánchez-Polo; José Rivera-Utrilla; Ozonation of 1,3,6-naphthalenetrisulphonic acid catalysed by activated carbon in aqueous phase. *Applied Catalysis B: Environmental* 2002, 39, 319-329, [10.1016/S0926-3373\(02\)00117-0](https://doi.org/10.1016/S0926-3373(02)00117-0).
8. Water. Sci. Technol.; Toxicity abatement and biodegradability enhancement of pulp mill bleaching effluent by advanced chemical oxidation. *Water Science and Technology* 1999, 40, 337-342, [10.1016/S0273-1223\(99\)00736-2](https://doi.org/10.1016/S0273-1223(99)00736-2).
9. Jun Ma; Nigel J.D. Graham; Preliminary Investigation of Manganese-Catalyzed Ozonation for the Destruction of Atrazine. *Ozone: Science & Engineering* 1997, 19, 227-240, [10.1080/01919519708547303](https://doi.org/10.1080/01919519708547303).
10. Méndez-Díaz, J.; Sánchez-Polo, M.; Rivera-Utrilla, J.; Bautista-Toledo, I.; Ferro-García, M.A. Ozonation in aqueous phase of sodium dodecylbenzenesulphonate in the presence of powdered activated carbon. *Carbon* 2005, 43, 3031–3034.
11. Rivera-Utrilla, J.; Méndez-Díaz, J.; Sánchez-Polo, M.; Ferro-García, M.A.; Bautista-Toledo, I. Removal of the surfactant sodium dodecylbenzenesulphate from water by simultaneous use of ozone and powdered activated carbon: Comparison with system based on O₃ and O₃/H₂O₂. *Water Res.* 2006, 40, 1717–1725.
12. Manuel Sánchez-Polo; J. Rivera-Utrilla; G. Prados-Joya; M.A. Ferro-García; I. Bautista-Toledo; José Rivera-Utrilla; Removal of pharmaceutical compounds, nitroimidazoles, from waters by using the ozone/carbon system. *Water Research* 2008, 42, 4163-4171, [10.1016/j.watres.2008.05.034](https://doi.org/10.1016/j.watres.2008.05.034).
13. José Rivera-Utrilla; Manuel Sánchez-Polo; Degradation and removal of naphthalenesulphonic acids by means of adsorption and ozonation catalyzed by activated carbon in water. *Water Resources Research* 2003, 39, 1232, [10.1029/2002wr001596](https://doi.org/10.1029/2002wr001596).
14. Johannes. Staehelin; Juerg. Hoigne; Decomposition of ozone in water in the presence of organic solutes acting as promoters and inhibitors of radical chain reactions. *Environmental Science & Technology* 1985, 19, 1206-1213, [10.1021/es00142a012](https://doi.org/10.1021/es00142a012).
15. M. Sánchez-Polo; R. Leyva-Ramos; J. Rivera-Utrilla; Kinetics of 1,3,6-naphthalenetrisulphonic acid ozonation in presence of activated carbon. *Carbon* 2005, 43, 962-969, [10.1016/j.carbon.2004.11.027](https://doi.org/10.1016/j.carbon.2004.11.027).
16. Mark E. Morgan; Robert G. Jenkins; Philip L. Walker Jr.; Inorganic constituents in American lignites. *Fuel* 1981, 60, 189-193, [10.1016/0016-2361\(81\)90176-9](https://doi.org/10.1016/0016-2361(81)90176-9).
17. C. Moreno-Castilla; F. Carrasco-Marín; F.J. Maldonado-Hódar; J. Rivera-Utrilla; Effects of non-oxidant and oxidant acid treatments on the surface properties of an activated carbon with very low ash content. *Carbon* 1998, 36, 145-151, [10.1016/S0008-6223\(97\)00171-1](https://doi.org/10.1016/S0008-6223(97)00171-1).
18. Michael S. Elovitz; Urs Von Gunten; Hydroxyl Radical/Ozone Ratios During Ozonation Processes. I. The RctConcept. *Ozone: Science & Engineering* 1999, 21, 239-260, [10.1080/01919519908547239](https://doi.org/10.1080/01919519908547239).
19. M. Sánchez-Polo; Urs Von Gunten; J. Rivera-Utrilla; Efficiency of activated carbon to transform ozone into OH radicals: Influence of operational parameters. *Water Research* 2005, 39, 3189-3198, [10.1016/j.watres.2005.05.026](https://doi.org/10.1016/j.watres.2005.05.026).
20. Urs Von Gunten; Ozonation of drinking water: Part II. Disinfection and by-product formation in presence of bromide, iodide or chlorine. *Water Research* 2003, 37, 1469-1487, [10.1016/S0043-1354\(02\)00458-X](https://doi.org/10.1016/S0043-1354(02)00458-X).
21. José Rivera-Utrilla; Manuel Sánchez-Polo; Ozonation of Naphthalenesulphonic Acid in the Aqueous Phase in the Presence of Basic Activated Carbons. *Langmuir* 2004, 20, 9217-9222, [10.1021/la048723+](https://doi.org/10.1021/la048723+).
22. M. Sánchez-Polo; José Rivera-Utrilla; Ozonation of naphthalenetrisulphonic acid in the presence of activated carbons prepared from petroleum coke. *Applied Catalysis B: Environmental* 2006, 67, 113-120, [10.1016/j.apcatb.2006.04.011](https://doi.org/10.1016/j.apcatb.2006.04.011).
23. Carlos Moreno-Castilla; Francisco Maldonado-Hódar; José Rivera-Utrilla; Enrique Rodríguez-Castellón; Group 6 metal oxide-carbon aerogels. Their synthesis, characterization and catalytic activity in the skeletal isomerization of 1-butene. *Applied Catalysis A: General* 1999, 183, 345-356, [10.1016/S0926-860X\(99\)00068-X](https://doi.org/10.1016/S0926-860X(99)00068-X).

24. Wencui Li; G Reichenauer; J Fricke; Carbon aerogels derived from cresol–resorcinol–formaldehyde for supercapacitors. *Carbon* **2002**, *40*, 2955-2959, [10.1016/s0008-6223\(02\)00243-9](https://doi.org/10.1016/s0008-6223(02)00243-9).
25. H Rotter; Miron V. Landau; M Carrera; D Goldfarb; Moti Herskowitz; High surface area chromia aerogel efficient catalyst and catalyst support for ethylacetate combustion. *Applied Catalysis B: Environmental* **2004**, *47*, 111-126, [10.1016/j.apcatb.2003.08.006](https://doi.org/10.1016/j.apcatb.2003.08.006).
26. Manuel Sánchez-Polo; J. Rivera-Utrilla; Urs Von Gunten; José Rivera-Utrilla; Metal-doped carbon aerogels as catalysts during ozonation processes in aqueous solutions. *Water Research* **2006**, *40*, 3375-3384, [10.1016/j.watres.2006.07.020](https://doi.org/10.1016/j.watres.2006.07.020).
27. Manuel Sánchez-Polo; J. Rivera-Utrilla; J. Méndez-Díaz; J. López-Peñalver; Metal-Doped Carbon Aerogels. New Materials for Water Treatments. *Industrial & Engineering Chemistry Research* **2008**, *47*, 6001-6005, [10.1021/ie8002039](https://doi.org/10.1021/ie8002039).
28. C.C David Yao; Werner R Haag; Rate constants for direct reactions of ozone with several drinking water contaminants. *Water Research* **1991**, *25*, 761-773, [10.1016/0043-1354\(91\)90155-j](https://doi.org/10.1016/0043-1354(91)90155-j).
29. Andreozzi, R.; Insola, A.; Caprio, V.; D'Amore, G.; The kinetics of Mn(II)-catalysed ozonation of oxalic acid in aqueous solution. *Water Res.* **1992**, *26*, 917–921, [0.1016/0043-1354\(92\)90197-C](https://doi.org/10.1016/0043-1354(92)90197-C).
30. Ma, J.; Graham, N.J.D.; Degradation of atrazine by manganese-catalysed ozonation-influence of radical scavengers. *Water Res.* **2000**, *34*, 3822–3828, .
31. Berend Smit; Theo L. M. Maesen; Towards a molecular understanding of shape selectivity. *Nature* **2008**, *451*, 671-678, [10.1038/nature06552](https://doi.org/10.1038/nature06552).
32. Valdés, H.; Farfán, V.J.; Manoli, J.A.; Zaror, C.A. Catalytic ozone aqueous decomposition promoted by natural zeolite and volcanic sand. *J. Hazard. Mater.* 2009, *165*, 915–922.
33. Sagehashi, M.; Shiraishi, K.; Fujita, H.; Fujii, T.; Sakoda, A. Adsorptive ozonation of 2-methylisoborneol in natural water with preventing bromate formation. *Water Res.* 2005, *39*, 3900–3908.
34. Sano, N.; Yamamoto, T.; Yamamoto, D.; Kim, S.-I.; Eiad-Ua, A.; Shinomiya, H.; Nakaiwa, M. Degradation of aqueous phenol by simultaneous use of ozone with silica-gel and zeolite. *Chem. Eng. Process.* 2007, *46*, 513–519.
35. J. Rivera-Utrilla; Manuel Sánchez-Polo; M.I. Bautista-Toledo; J.D. Méndez-Díaz; Enhanced oxidation of sodium dodecylbenzenesulfonate aqueous solution using ozonation catalyzed by base treated zeolite. *Chemical Engineering Journal* **2012**, *180*, 204-209, [10.1016/j.cej.2011.11.050](https://doi.org/10.1016/j.cej.2011.11.050).
36. Fernando J. Beltrán; Juan F. García-Araya; Pedro M. Álvarez; Sodium Dodecylbenzenesulfonate Removal from Water and Wastewater. 1. Kinetics of Decomposition by Ozonation. *Industrial & Engineering Chemistry Research* **2000**, *39*, 2214-2220, [10.1021/ie990721a](https://doi.org/10.1021/ie990721a).
37. Urs Von Gunten; Ozonation of drinking water: Part I. Oxidation kinetics and product formation. *Water Research* **2003**, *37*, 1443-1467, [10.1016/s0043-1354\(02\)00457-8](https://doi.org/10.1016/s0043-1354(02)00457-8).

Retrieved from <https://encyclopedia.pub/entry/history/show/14357>